



**HAL**  
open science

## High Clouds over Oceans in the ECMWF 15- and 45-Yr Reanalyses

Frederic Chevallier, Graeme Kelly, Adrian Simmons, Sakari Uppala, Angeles Hernandez

► **To cite this version:**

Frederic Chevallier, Graeme Kelly, Adrian Simmons, Sakari Uppala, Angeles Hernandez. High Clouds over Oceans in the ECMWF 15- and 45-Yr Reanalyses. *Journal of Climate*, 2005, 18 (14), pp.2647-2661. 10.1175/JCLI3429.1 . hal-02957383

**HAL Id: hal-02957383**

**<https://hal.science/hal-02957383>**

Submitted on 13 Feb 2021

**HAL** is a multi-disciplinary open access archive for the deposit and dissemination of scientific research documents, whether they are published or not. The documents may come from teaching and research institutions in France or abroad, or from public or private research centers.

L'archive ouverte pluridisciplinaire **HAL**, est destinée au dépôt et à la diffusion de documents scientifiques de niveau recherche, publiés ou non, émanant des établissements d'enseignement et de recherche français ou étrangers, des laboratoires publics ou privés.

## High Clouds over Oceans in the ECMWF 15- and 45-Yr Reanalyses

FRÉDÉRIC CHEVALLIER,\* GRAEME KELLY, ADRIAN J. SIMMONS, SAKARI UPPALA, AND ANGELES HERNANDEZ

*European Centre for Medium-Range Weather Forecasts, Reading, United Kingdom*

(Manuscript received 12 December 2003, in final form 12 May 2004)

### ABSTRACT

The reanalysis programs of numerical weather prediction (NWP) centers provide global, comprehensive descriptions of the atmosphere and of the earth's surface over long periods of time. The high realism of their representation of key NWP parameters, like temperature and winds, implies some realism for less emblematic parameters, such as cloud cover, but the degree of this realism needs to be documented.

This study aims to evaluate the high clouds over open oceans in the ECMWF 15- and 45-yr reanalyses. The assessment is based on a new 23-yr climatology of monthly frequencies of high-cloud occurrence retrieved from the infrared radiances measured by operational polar satellites. It is complemented by data from the International Satellite Cloud Climatology Project.

It is shown that the 45-yr ECMWF reanalysis dramatically improves on the previous 15-yr reanalysis for the realism of seasonal and interannual variations in high clouds, despite remaining systematic errors. More than 60% of the observed anomalies during the January 1979–February 2002 period over large oceanic basins are captured by the latest reanalysis. However the realism of the analyses in the areas and in the years with sparse observations appears to be poor. Consequently, the interannual variations may not be reliable before January 1979 in most parts of the world. Possible improvements of the handling of assimilated satellite observations before and after this date are suggested.

### 1. Introduction

Growing concern about the evolution of the earth's climate has increased interest in understanding past atmospheric records. Time series of satellite observations are relatively short, but they are an interesting source of information because they cover wide portions of the globe. The measurements of the electromagnetic radiation emitted by the earth–atmosphere system at wavelengths around 11 and 14  $\mu\text{m}$  that have been operationally made by the polar-orbiting satellites of the National Oceanic and Atmospheric Administration (NOAA) cover an exceptionally long period for satellite data. The initial Vertical Temperature Profile Radiometer (VTPR) was operated on board four NOAA

satellites between November 1972 and February 1979. It was superseded by the High-Resolution Infrared Radiation Sounder (HIRS) in October 1978, which provided additional infrared channels and is still operated today. The next generation, for instance, the Atmospheric Infrared Sounder (AIRS), launched in 2002 by the National Aeronautics and Space Administration (NASA), achieves a much finer sampling of the infrared spectrum.

The extraction of consistent information about the atmosphere from this historical dataset, in spite of instrument and platform orbit changes, has mobilized considerable efforts [e.g., Susskind et al. (1997) and Scott et al. (1999) for the HIRS record]. Very few institutes can afford to integrate these observations together with conventional measurements in a global system. Consequently, the reanalysis programs from the National Centers for Environmental Prediction–National Center for Atmospheric Research (NCEP–NCAR), from the Data Assimilation Office (DAO), and from the European Centre for Medium-Range Weather Forecasts (ECMWF) have received much attention. Each program relies on a fixed assimilation and

---

\* Current affiliation: Laboratoire des Sciences du Climat et de l'Environnement, Gif sur Yvette, France.

---

*Corresponding author address:* Dr. F. Chevallier, Laboratoire des Sciences du Climat et de l'Environnement, Bat 701, L'Orme des Merisiers, 91191 Gif sur Yvette Cedex, France.  
E-mail: frederic.chevallier@cea.fr

forecasting system for the period that it covers, making it more homogeneous than the operational archives of the numerical weather prediction (NWP) centers. To date, ECMWF has run two reanalysis projects, in partnership with other institutes. The first one covered the December 1978–February 1994 period [15-yr ECMWF Re-Analysis (ERA-15; Gibson et al. 1997)] and the second one [45-yr ECMWF Re-Analysis (ERA-40; Simmons and Gibson 2000)] extended that period backward to September 1957 and forward to August 2002, using a more advanced data assimilation system.

This study aims to evaluate the realism of the high clouds over open oceans in both ECMWF reanalyses. Following the methodology defined by Chevallier et al. (2001), cloud-affected raw observations from HIRS serve as a reference for ERA-40 since those observations have not been assimilated. ERA-15 used some of them, but in the form of cloud-clear radiances. To help the interpretation, monthly frequencies of high clouds are estimated from the raw radiances with the CO<sub>2</sub>-slicing method of Wylie et al. (1994). This product not only serves as a validation reference, but is also of direct climatological significance.

The paper is divided into seven sections. Following the introduction, section 2 describes the model and satellite data. The frequencies of high clouds directly obtained from the HIRS observations are presented in section 3. In section 4 this new dataset, ERA-40, and corresponding data from the International Satellite Cloud Climatology Project (ISCCP; Rossow and Schiffer 1999) are intercompared. ERA-15 is then evaluated in section 5. A specific assessment of the pre-HIRS period of ERA-40 is presented in section 6. Concluding discussion follows in section 7.

## 2. The data

### a. ERA-15 and ERA-40

The ERA-15 and ERA-40 productions were mainly based on systems set up six years apart (1994 and 2000, respectively). Many features denote the scientific and technical progress of the ECMWF forecasting system achieved in between, and significant improvements of the skill of NWP have been demonstrated (Simmons and Hollingsworth 2002). Knowledge of the specifics of these changes is not needed to understand the results presented here. The reader is referred to Simmons and Gibson (2000) and to Simmons (2001) for a detailed list of the differences between the two systems in terms of spatial resolution, data assimilation system, advection formulation, physical parameterizations, assimilated observations, and external forcing. It is worth mentioning that two prognostic equations described the time

evolution of cloud condensate and cloud cover in both forecast models (Tiedtke 1993), but these variables were only diagnosed since the analysis control variables included vorticity, divergence, surface pressure, wind, temperature, and moisture only. Ozone was another control variable for ERA-40 only.

Two previous studies specifically documented some aspects of the quality of the clouds in both reanalyses. Jakob (1999) compared total cloud cover from ERA-15 and ISCCP. Chevallier et al. (2001) used infrared and microwave radiances to evaluate high, medium, and low clouds in one year of a preparatory ERA-40 run. For high clouds, they noted a systematic underestimation of their radiative forcing, likely caused by an underestimation of the cloud ice, and a too static intertropical convergence zone (ITCZ). The present study complements that by Chevallier et al. (2001) and is based on the full ERA-40 archive.

### b. HIRS

The HIRS instrument measures radiation in 20 channels covering both the longwave and shortwave parts of the spectrum to serve various purposes (Smith et al. 1979). Seven of them have a central wavelength between 13 and 15  $\mu\text{m}$  and allow the retrieval of atmospheric temperature in seven corresponding broad layers centered about 30, 60, 100, 400, 600, 800, and 900 hPa. Also of interest here is an 11- $\mu\text{m}$  atmospheric window channel.

The spacecrafts that carry this instrument orbit at about 850-km altitude from pole to pole and in synchronization with the sun. The orbits actually drift during the lifetime of the satellites, in particular for those that were positioned to cross the equator northbound in the local solar afternoon (Price 1991). The series of NOAA satellites that followed one another with HIRS on board and the drift of their orbits appear in Fig. 1. The drift of *NOAA-11* is particularly large. *NOAA-11* was brought to a 1340 LST orbit after launch in September 1988 and had reached a 2145 LST orbit by April 2000 when its HIRS instrument failed.

The HIRS ground instantaneous field of view (FOV) is typically a circle of 17-km diameter at nadir. At the end of the scan, 50° from nadir, the FOV covers 58 km cross track by 30 km along track (Kidwell 1998). The HIRS FOV from *NOAA-15* and *NOAA-16* is slightly larger (Goodrum et al. 2000).

### c. Radiance calibration

Cloud-affected HIRS radiances serve here as a reference for the evaluation of the quality of ERA-15 and ERA-40. It is therefore useful to summarize the steps

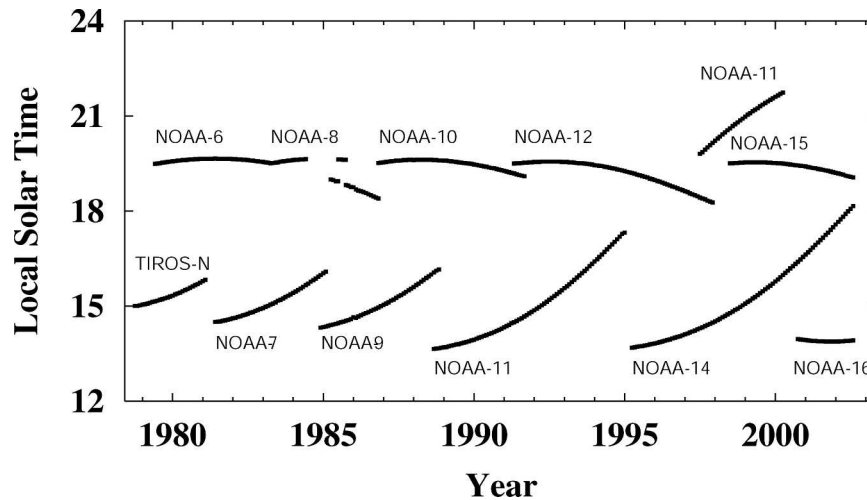


FIG. 1. Local solar time of the ascending node (northbound equator crossing) of the NOAA satellite series.

of their processing at ECMWF. Hernandez et al. (2004) describe the in-house calibration of the HIRS (until *NOAA-14*) radiance counts for ERA-40. *NOAA-15* and *NOAA-16* radiances were calibrated by the U.K. Met Office. The data were further bias-corrected with respect to the NWP first-guess radiance simulations using the method described by Harris and Kelly (2001). The scheme takes into account the biases from the instruments, those from the NWP first-guess fields, and those from the radiance model. Its parameters are estimated on a large sample of data, usually covering a couple of weeks, during which the instrument is passively monitored in the NWP system (i.e., during which it is not assimilated).

As mentioned in the introduction, the HIRS cloud-affected observations have been passively monitored in the ERA-40 system but *have not been assimilated*, not even in the form of a cloud-cleared product. To reduce the data load, only one HIRS spot in four was kept.

#### d. ISCCP

A complementary assessment of the quality of ERA-40 is provided by the ISCCP climatology. As described by Rossow and Schiffer (1999), the latter involves an analysis of the  $0.6\text{-}\mu\text{m}$  and  $11\text{-}\mu\text{m}$  radiances observed by imagers on board operational geostationary and polar-orbiting satellites. The ISCCP radiance calibration procedure is reported by Brest et al. (1997). ISCCP is a comprehensive global dataset of cloud variables at varying spatial and temporal resolutions. Two ISCCP parameters, the monthly high cloud amount and the monthly total cloud amount from the D2 “vis-adjusted” product, are utilized in this study in an equal-area map

form. Data from July 1983 to September 2001 were available at the time of writing.

### 3. Retrieval of high cloud frequency from HIRS

#### a. The retrieval method

Cloud-top pressures are retrieved from HIRS radiances using a  $\text{CO}_2$ -slicing method (e.g., Chahine 1974). The present algorithm is described by Wylie et al. (1994). The cloud statistics compiled at the University of Wisconsin (UW) using this technique have been extensively studied and compared to other climatologies (Wylie et al. 1994; Jin et al. 1996; Wylie and Wang 1997; Wylie and Menzel 1999). The algorithm is summarized as follows.

For each HIRS spot the temperature profile, the absorbing gas profiles, and the surface temperature are defined a priori from an external data source: ERA-40 short-range (3–9 h) forecasts in this study. From these variables, a radiation model, here the Radiative Transfer for Television Infrared Observation Satellite (TIROS) Operational Vertical Sounder (RTTOV; Eyre 1991; Saunders et al. 1999), calculates a series of radiation quantities, like the model clear-sky radiances. A preliminary cloud detection is based on the  $11\text{-}\mu\text{m}$  window channel: if the difference between the observed and the background clear-sky radiance does not exceed some threshold, the spot is declared to be clear. Alternatively, the impact of cloudiness on the radiances in the  $13\text{--}15\text{-}\mu\text{m}$   $\text{CO}_2$  absorption band is modeled by two variables: a cloud top pressure  $P_{\text{top}}$  and a channel-dependent cloud effective emissivity  $n\varepsilon_v$ , where  $n$  is the fractional area cloud cover and  $\varepsilon_v$  is the cloud emissiv-

ity. Scattering is ignored and unit surface emissivity is assumed. If the variations of  $n\varepsilon_\nu$  between two spectrally close channels are neglected,  $P_{\text{top}}$  and  $n\varepsilon_\nu$  are uniquely defined for this pair. The  $\text{CO}_2$ -slicing algorithm is consequently run for four HIRS channel pairs in the 13–15- $\mu\text{m}$  band. A quality control selects the most likely  $P_{\text{top}}/n\varepsilon_\nu$  association or rejects the retrieval. In the latter case the algorithm returns an estimation based solely on the 11- $\mu\text{m}$  channel assuming unity cloud emissivity  $n\varepsilon_\nu$ , that is, overcast and optically dense cloud.

The quality of the prior information (i.e., the atmospheric and surface temperatures and the absorbing gas profiles) obviously affects the quality of the retrieval. In particular, if that prior information is biased, the retrieval will be as well. It may be noted that in this context, the principle of the bias correction scheme used here, which tackles both instrumental and model biases, is appropriate. The high cloud statistics shown here are marginally affected by errors in the atmospheric component of the prior information. For instance, replacing the short-range forecasts by a climate simulation (therefore much less realistic, see section 6 below) changes the monthly high cloud occurrences by about 2% only in root-mean-square difference. In contrast, the surface temperature plays an important role since it controls the cloud detection and therefore triggers, or not, the retrieval of  $P_{\text{top}}$  and  $n\varepsilon_\nu$ . Consequently, data are processed neither over land nor over sea ice, where the ERA-40 surface temperature is not judged to be of good enough quality for the retrieval. The sea surface temperature dataset is an external forcing to ERA-40, based on state-of-the-art reanalyses of satellite and conventional observations as described by Fiorino (2004).

#### b. A new database of satellite-based cloud statistics

Cloud-top pressure and cloud effective emissivity retrievals have been performed for the whole ERA-40 HIRS archive. Individual retrievals are further classified into three cloud types that follow the ISCCP convection (Rossow and Schiffer 1999): high ( $P_{\text{top}} < 440$  hPa), medium ( $440 \text{ hPa} \leq P_{\text{top}} < 680$  hPa), and low ( $P_{\text{top}} \geq 680$  hPa).

Monthly frequencies of high, medium, and low cloud occurrence over ocean in a regular  $2.5^\circ$  equal angle grid have been compiled separately for each satellite for the periods during which its cloud-free observations were assimilated in the ERA-40 system (i.e., the periods during which the radiance bias correction was set). HIRS viewing angles larger than  $41^\circ$  have been removed since we found that nonlinear variations of the retrieved high cloud occurrence with respect to viewing angle caused excessive weight for them in the monthly statistics.

An interesting illustration of the quality of the dataset is shown in Fig. 2, with the series of monthly high cloud occurrences in three broad latitude bands. Most satellite curves overlap with each other with mean differences less than 1%, even those in very different orbits, like *NOAA-9* and *NOAA-10*. This highlights the efficacy of the radiance bias correction scheme. The corresponding standard deviations are about 6% (not shown). However, some outliers can be noticed: *NOAA-8* and the last three platforms (*NOAA-14*, *NOAA-15*, and *NOAA-16*). There is no known reason for this, and better agreement could arguably be obtained in a future reanalysis of the data from these satellites. *NOAA-14* actually agrees with *NOAA-12* after 1 January 1997, on which date the ERA-40 radiance bias correction coefficients were updated.

In the following, the high cloud statistics from all individual instruments are compiled in a single time series by excluding the problematic ones, that is, *NOAA-8*, *NOAA-14* before 1 January 1997, *NOAA-15*, and *NOAA-16*. This new climatology covers the period from January 1979 to February 2002. Since it incorporates some information from ERA-40 (i.e., the bias correction scheme, the atmospheric and surface temperature, and the gas profiles), it is not strictly independent from the ECMWF reanalyses. However, the impact of the quality of this contribution on the climatology, which uses the best calibrated satellites only, is believed to be small (see section 3a).

#### c. Corresponding definition of high clouds for ERA-15 and ERA-40

Satellite retrievals obviously depend on the sensitivity of the observing instrument. For instance, differences between the Stratospheric Aerosol and Gas Experiment II (SAGE II), ISCCP, and the HIRS UW cloud climatologies were attributed to different sensitivities of the respective instruments (Liao et al. 1995; Jin et al. 1996). Therefore, the comparison between cloud-top pressure retrievals and simulated cloud profiles is not straightforward. Chevallier et al. (2001) suggested using the model fields to compute the radiances in the satellite channels at the same location and time as the observations and to process them with the same cloud retrieval algorithm. This approach has been applied for the present study. Radiance computations are performed from a version of RTTOV that has been extended to treat multilayer cloudiness (Chevallier et al. 2001). Importantly, the cloud optical properties and the cloud overlap scheme are consistent with those of the ECMWF model (Morcrette et al. 2001). This “HIRS simulator” allows a rigorous evaluation of the model, but it involves collocating the model fields and

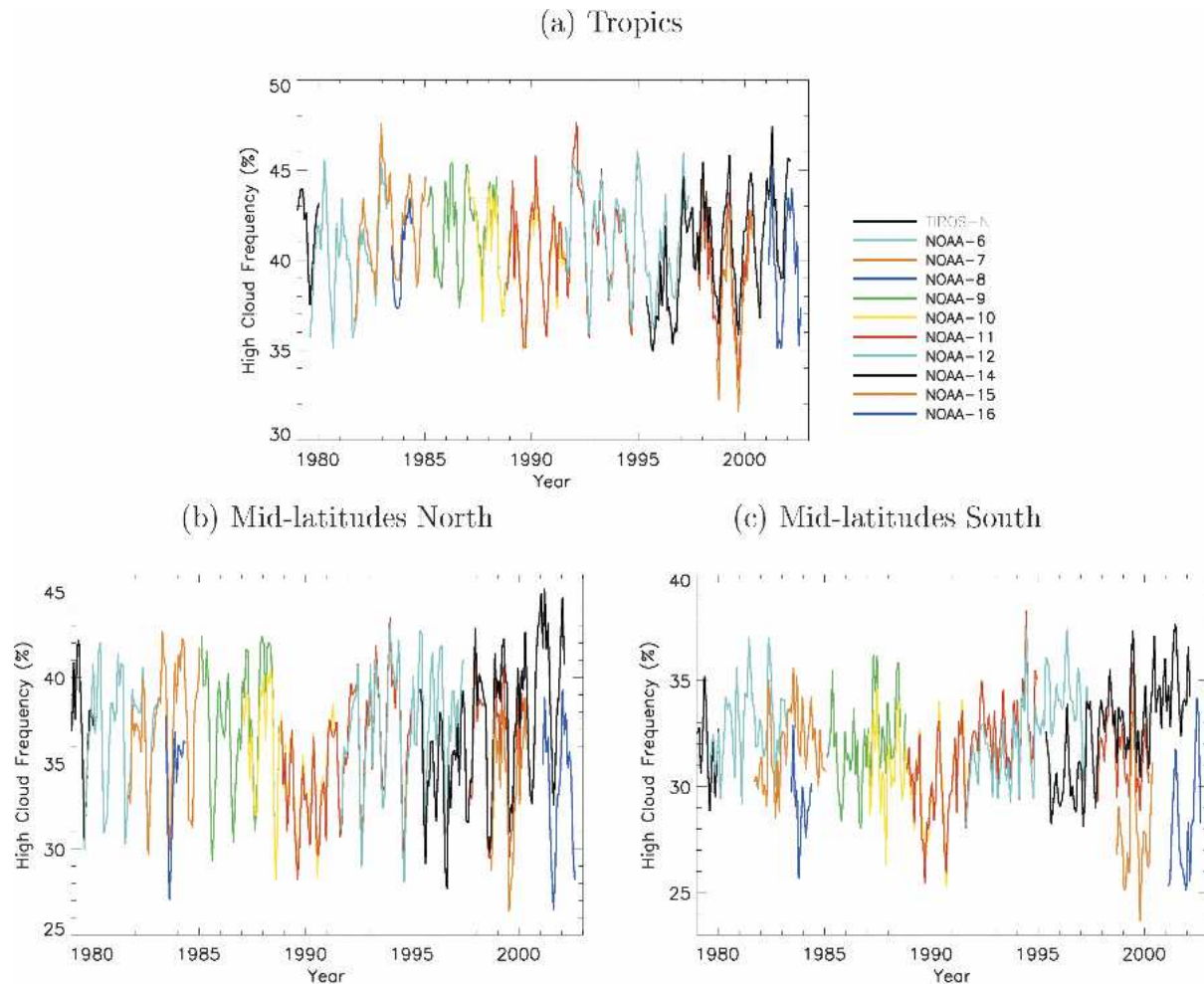


FIG. 2. Frequency of high clouds in the Tropics ( $15^{\circ}\text{S}$ – $15^{\circ}\text{N}$ ), northern midlatitudes ( $30^{\circ}$ – $50^{\circ}\text{N}$ ), and southern midlatitudes ( $30^{\circ}$ – $50^{\circ}\text{S}$ ). The distinction is made between the estimation from each individual satellite. Statistics for a particular platform and a particular month were computed when data are regularly spread in both time and space throughout the month for that platform. Data of suspicious quality, as indicated by the ERA-40 “blacklist” files, were removed.

the observations both spatially and temporally. Moreover, the interpolation in time is best performed on short-range forecasts (with a subhour time step) rather than on analyses performed 6 hours apart. Therefore, the radiance computations used here for ERA-40 have been done with the short-range forecast model (i.e., between 3 and 9 h depending on observation time) directly within the ERA-40 processing and are part of the archive. This dataset is used in section 4 and is simply referred to as “ERA-40” in that section.

To process other data more easily, like ERA-15, as is done in sections 5 and 6, a simpler high cloud detection is defined. A high cloud is diagnosed when the mean cloud ice column in the model grid box above 440 hPa exceeds  $0.002 \text{ kg m}^{-2}$  within  $30^{\circ}$  latitude from the equator and  $0.005 \text{ kg m}^{-2}$  elsewhere. The mean cloud ice contents in the model grid box are computed by mul-

tipling the layer cloud ice contents by the layer fractional cloud covers. Global model fields are processed at the temporal resolution of the archive (every 6 hours for ERA-15 and ERA-40 analyses; every 12 hours for medium and long ERA-40 ranges, except where indicated), without any reference to the observation date and location. This simplification would not be appropriate over land. The quality of the high cloud occurrence based on this empirical cloud detection is evaluated in section 5.

#### 4. Comparison between ERA-40, HIRS, and ISCCP

##### a. Expected differences

The high clouds in the ERA-40 short-range forecasts are compared to HIRS retrievals and to the ISCCP

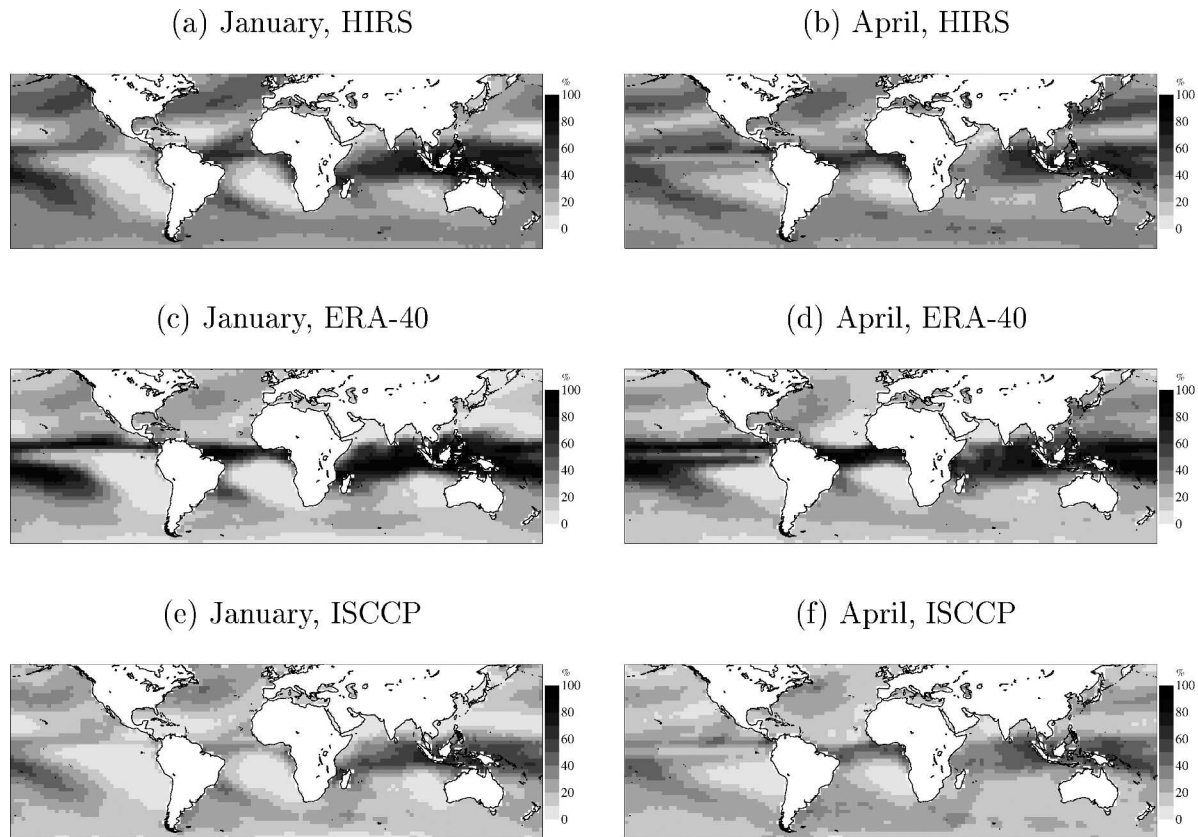


FIG. 3. Mean frequency of high clouds from HIRS, ERA-40, and ISCCP for Jan and Apr between Jul 1983 and Sep 2001.

climatology. It is well known that ISCCP and HIRS-based climatologies have different sensitivities to thin cirrus, which results in more high clouds in the HIRS-based datasets (Jin et al. 1996; Stubenrauch et al. 1999). As for ERA-40, the HIRS-like postprocessing of the model data described in the previous section is intended to make it close to HIRS rather than to ISCCP. However, it should be noted that size differences between ERA-40 grid points (125 km) and HIRS spots (less than 60 km) induce small irreducible differences in terms of cloud frequencies. For instance, Chevallier et al. (2003) showed that the HIRS-retrieved cloud occurrences were about 5% smaller than those from VTPR, whose ground FOV covers an area about 10 times as large. In that case, no particular latitude dependency of that shift was observed.

#### b. Mean annual cycle

Figures 3 and 4 present the mean high cloud frequencies for January, April, July, and October between July 1983 and September 2001. Annual mean values in the 10 large regions defined in Table 1 are given in Table

2. HIRS and ERA-40 frequencies are larger than those shown by Chevallier et al. (2001) due to a revision of the implementation of the CO<sub>2</sub>-slicing algorithm. The three datasets grossly agree with each other for the broad patterns of the midlatitude storm tracks and of the intertropical South Pacific and South Atlantic (e.g., Liebmann et al. 1999) convergence zones. One example is the double structure of the ITCZ that exists during some boreal springs in the eastern Pacific (e.g., Hubert et al. 1969) and that appears in the three April monthly means. Despite the particularly good agreement between HIRS and ISCCP for the horizontal patterns, occurrences are smaller in ISCCP due to different sensitivities to thin cirrus (see section 4a): in Table 2, the ISCCP/HIRS ratio ranges from 56% (southern Indian Ocean) to 74% (tropical Indian Ocean). One may notice a large circular pattern in the western Indian Ocean at about longitude 60°E for ISCCP. It is located about the border of the disk of the Meteosat satellite stationed close to 0° longitude and may indicate some remaining calibration issue for this database as well.

Consistent with previous results (Chevallier et al. 2001), the ERA-40 ITCZ appears too static and fre-

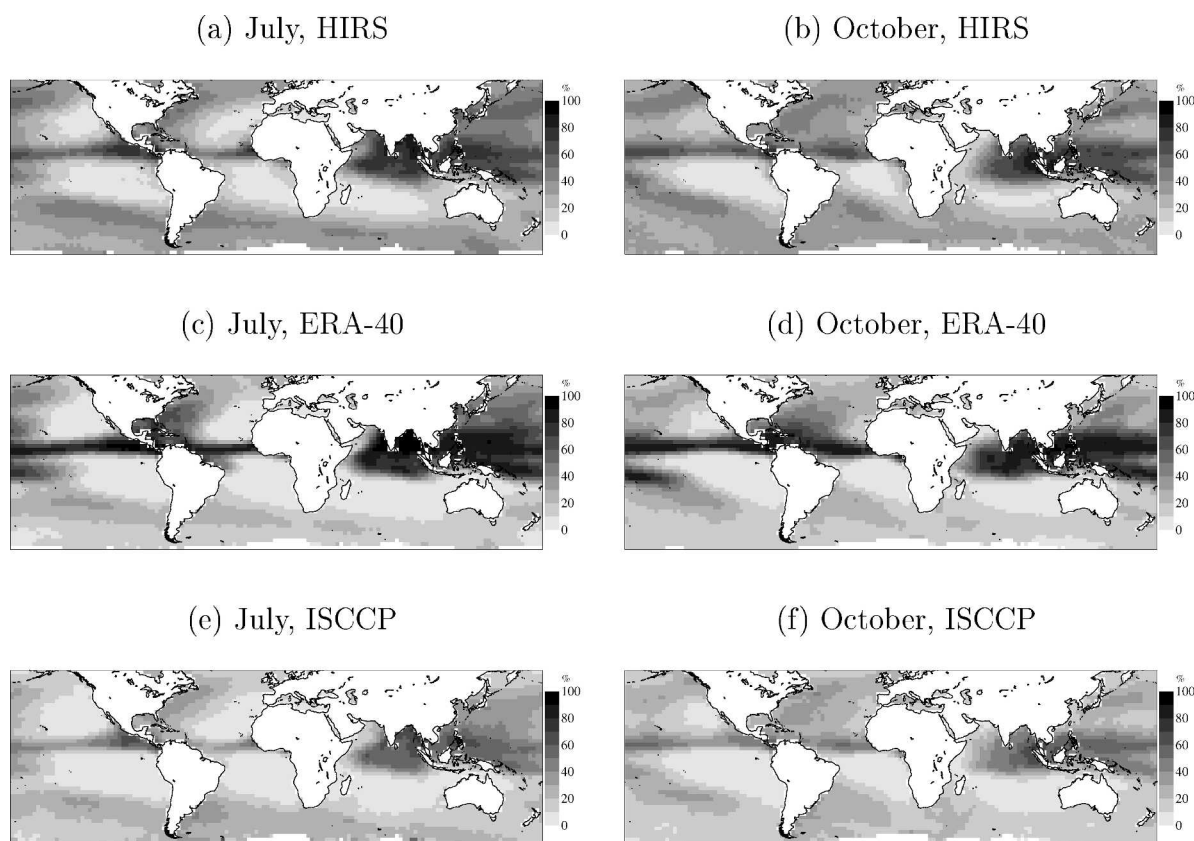


FIG. 4. As in Fig. 3 but for Jul and Oct.

quencies seem to be underestimated in the midlatitudes: the ERA-40/HIRS ratio is about 1.1, 0.8, and 0.5 in the tropical regions, in the northern midlatitudes, and in the southern midlatitudes, respectively. One may note as well that the seasonal cycle around the tropic of Cancer is not adequately represented in the western Pacific, with too-large values north of the ITCZ in April and an excessive northern ITCZ extent in July and October. Last, the northern Atlantic storm-track pattern in July and October reproduces neither ISCCP nor HIRS along the east coast of America.

TABLE 1. Definition of the maritime regions used.

Region	Boundaries		Symbol
Tropical Atlantic	20°S–20°N	60°W–20°E	b
Tropical Indian	20°S–20°N	50°E–100°E	c
Indonesia	20°S–20°N	100°E–140°E	d
Tropical western Pacific	20°S–20°N	140°E–180°E	e
Tropical eastern Pacific	20°S–20°N	180°E–100°W	h
Northern Atlantic	20°–60°N	70°W–0°	k
Northern Pacific	30°–60°N	160°E–140°E	m
Southern Atlantic	60°–30°S	70°W–20°E	p
Southern Indian	60°–30°S	20°E–140°E	s
Southern Pacific	60°–30°S	140°E–170°E	v

### c. Interannual anomalies

In the context of a changing climate, much focus has been put on trend estimation (e.g., Houghton et al. 2001). Through their data assimilation systems, the re-analyses from NWP centers capture some of the observation temporal variability. Interannual anomalies from ERA-40, HIRS, and ISCCP are compared in this section. They are computed for each dataset by remov-

TABLE 2. Annual mean frequency of high clouds from HIRS, ERA-40, ISCCP, and the climate run between Jul 1983 and Sep 2001 in the 10 maritime regions defined in Table 1.

Region	HIRS	ERA-40	ISCCP	Climate run
Tropical Atlantic	27.7	29.2	16.9	24.7
Tropical Indian	43.8	51.6	32.5	42.5
Indonesia	50.8	55.6	36.0	38.2
Tropical western Pacific	52.8	62.5	37.6	52.2
Tropical eastern Pacific	30.5	38.5	19.5	34.2
Northern Atlantic	32.6	27.1	20.8	28.4
Northern Pacific	30.1	22.0	18.1	25.6
Southern Atlantic	33.9	18.7	23.2	25.9
Southern Indian	29.7	15.2	16.7	23.5
Southern Pacific	32.4	17.9	18.6	27.2

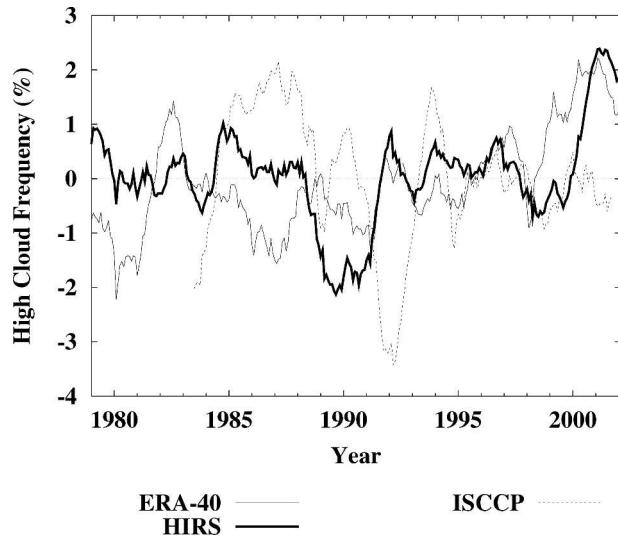


FIG. 5. Mean high cloud frequency anomalies over  $60^{\circ}\text{S}$ – $60^{\circ}\text{N}$  oceans from ERA-40, HIRS, and ISCCP. Monthly anomalies are defined for each dataset with respect to its Jul 1983–Sep 2001 climatology. Curves have been smoothed with a two-sided exponentially weighted average.

ing the mean annual cycles previously shown in Figs. 3 and 4.

Figure 5 presents the mean cloud frequency anomalies for high clouds over the oceans between  $60^{\circ}\text{S}$  and  $60^{\circ}\text{N}$ . Time series have been smoothed with a two-sided exponentially weighted average to ease the visualization. The differences between the datasets make it difficult to conclude on the actual trends of the atmosphere. The largest disagreement between HIRS and ISCCP concerns the 1991–92 period. It corroborates

the results of Luo et al. (2002), who compared ISCCP and two separate cloud datasets, including another HIRS-based climatology (Scott et al. 1999), for the same period and concluded that the volcanic aerosols spread by the Mt. Pinatubo eruption in June 1991 induced a misclassification of thin cirrus in ISCCP. The reasons for other disagreements, like in 1985, in 1989–90, or at the end of the record, are not obvious. For instance, it has not been possible to link them with any change in the ERA-40 processing or with the availability of the various observation sources. ERA-40 differs from HIRS in the 1980s but reproduces its main patterns between 1991 and 1998. Both datasets describe an increase afterward, but the fact that it occurs one to two years too early in ERA-40 may indicate that the lagged agreement is fortuitous.

For further comparison of the high cloud trends, the globe ocean surface is divided into the 10 regions shown in Table 1. The difference between ISCCP and HIRS and between ERA-40 and HIRS, are displayed in Fig. 6 with the polar representation proposed by Taylor (2001). The radial axis indicates the standard deviation of one of the datasets normalized with that of the other, while the angular axis indicates the correlation between the two datasets concerned. HIRS is the reference for the two diagrams in Fig. 6 and consequently appears on the graphs at location (1, 1), that is, with a unity normalized standard deviation and a unity correlation. The differences of the other dataset (ISCCP in Fig. 6a and ERA-40 in Fig. 6b) with the reference are visualized by letters symbolizing the 10 maritime regions studied. By construction, the distance between those points on the

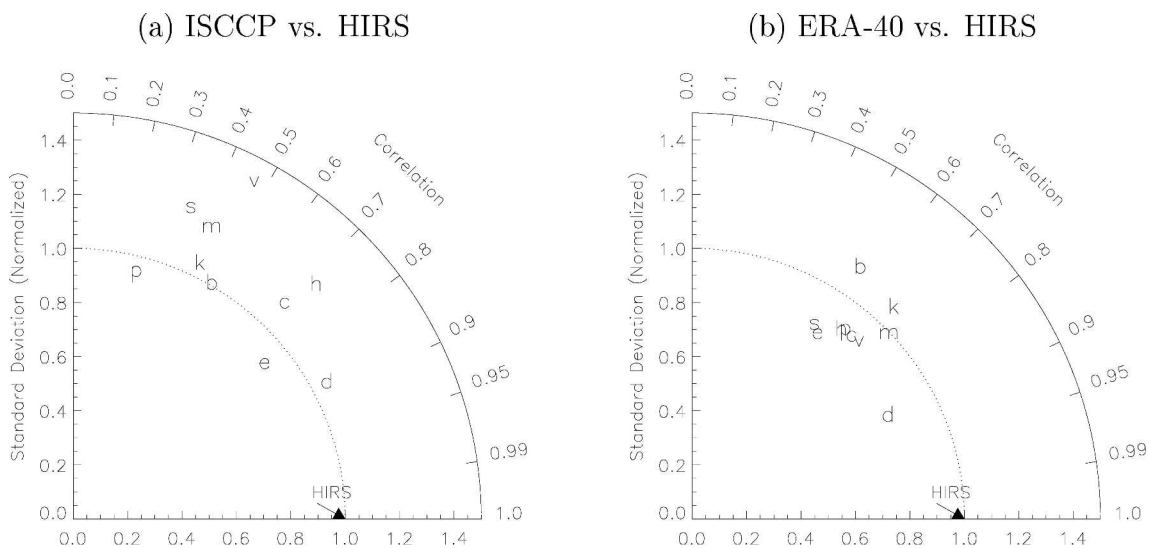


FIG. 6. Polar representation of normalized standard deviations (radius) vs correlations (angle) between the high cloud frequency anomalies from HIRS and (left) from ISCCP or (right) from ERA-40. Monthly anomalies are defined for each dataset with respect to its Jul 1983–Sep 2001 climatology. Statistics are computed for the 10 maritime regions of Table 1.

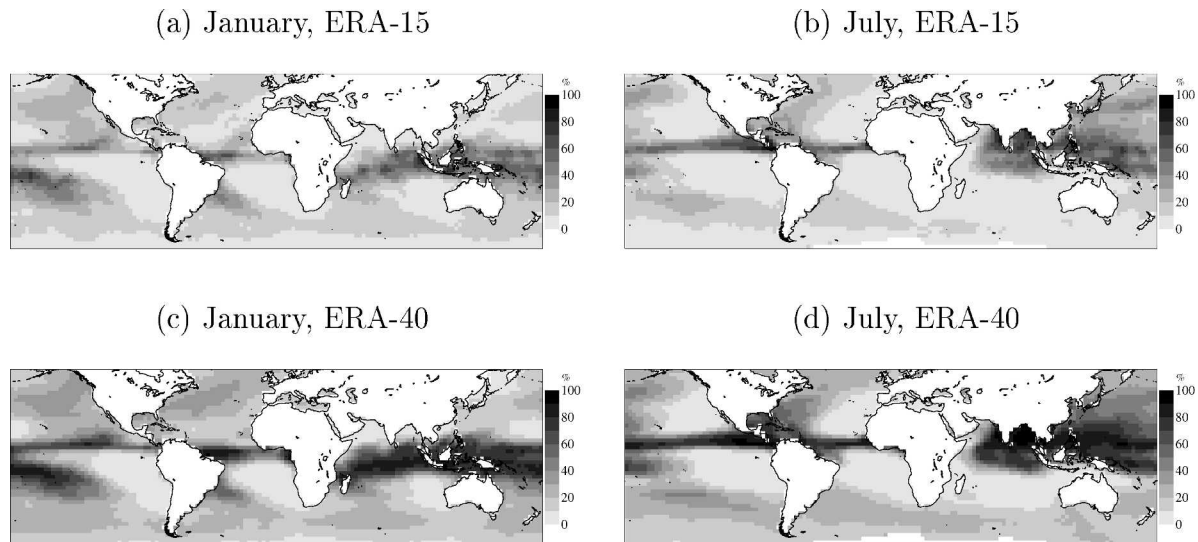


FIG. 7. Mean frequency of high clouds from ERA-15 and ERA-40 analyses for Jan and Jul between Jan 1979 and Dec 1993 for both ERA-15 and ERA-40; high clouds are detected from the cloud ice profiles.

graph and the reference at location (1, 1) is a normalized standard deviation of the differences between the two datasets (Taylor 2001).

As expected (see section 4a), Fig. 6a shows a large spread of the differences between ISCCP and HIRS. Correlations are 0.6 for the tropical regions from the Indian to the eastern Pacific only, regions that are dominated by the Indian monsoon circulation and the El Niño–Southern Oscillation (ENSO). For other regions, the two datasets are only weakly correlated (the correlation is about 0.4) and seem not to describe the same variations of the atmosphere.

As detailed before, ERA-40 has been postprocessed to reproduce the HIRS-like climatology, and indeed the correlations between ERA-40 and HIRS, with values above 0.5 for all regions, are noticeably positive. The correlations are even larger (above 0.6) when the comparison is extended to the 23 years of the HIRS database (not shown). The ERA-40 anomaly amplitude is also close to HIRS with normalized standard deviations between 0.8 and 1.2, but usually smaller than 1, as can be expected from the underestimation of high cloud occurrence in the extratropics.

### 5. Evaluation of ERA-15

As discussed in section 3d, a simple threshold method is used to postprocess ERA-15, rather than the elaborate HIRS simulator. The impact of this simplification can be seen in Figs. 7c, 7d and 8 for ERA-40. The high cloud seasonal cycle (Figs. 7c and 7d, to be compared with Figs. 3c and 4c, respectively) is marginally

affected. The normalized standard deviations are slightly degraded, by up to 0.1 (Fig. 8). The anomaly correlations are not much affected in three of the regions and are degraded by up to 0.1 in the other ones.

The high clouds appears to have been dramatically improved between ERA-15 and ERA40 (Fig. 7 and Table 3), with increased contrast between the regions of ascent (where the frequencies of high clouds increase

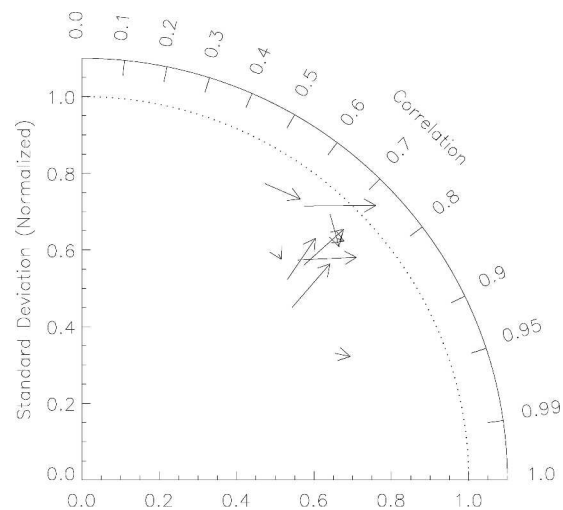


FIG. 8. Polar representation of normalized standard deviations (radius) vs correlations (angle) between the high cloud frequency anomalies from HIRS and ERA-40 using the analysis cloud ice profiles (tail of the arrows) or the radiance computation (head of the arrows). Monthly anomalies are defined for each dataset with respect to its Jan 1979–Dec 1993 climatology. Statistics are computed for the 10 maritime regions of Table 1, but for clarity the arrows are not labeled.

TABLE 3. Annual mean frequency of high clouds from ERA-15 and ERA-40 analyses between Jan 1979 and Dec 1999 in the 10 maritime regions defined in Table 1. For both ERA-15 and ERA-40, high clouds are detected from the cloud ice profiles.

Region	ERA-15	ERA-40
Tropical Atlantic	15.3	26.9
Tropical Indian	28.6	46.8
Indonesia	33.2	51.1
Tropical western Pacific	38.7	58.4
Tropical eastern Pacific	22.5	35.5
Northern Atlantic	15.9	26.8
Northern Pacific	15.5	24.1
Southern Atlantic	12.9	21.3
Southern Indian	10.0	18.3
Southern Pacific	12.3	21.6

by about 10% from ERA-15 to ERA-40) and descent (where numbers are stable). A detrimental side effect can be seen around the tropic of Cancer in the western Pacific, where the ERA-40 ITCZ erroneously extends more northward than in ERA-15 in summer.

The anomalies displayed in Fig. 9 also show an improved realism from ERA-15 to ERA-40 in all regions but one, with correlations about 0.1 higher in ERA-40 while the normalized standard deviations are stable. The exception is the tropical western Pacific area where the ERA-40 signal amplitude is 0.2 farther away from the reference, compared to ERA-15.

## 6. ERA-40 before HIRS

So far, this study has only focused on the evaluation of the ECMWF reanalyses for the HIRS period. It has

therefore covered the full ERA-15 record but only half of the ERA-40 archive, which starts in 1957. Chevallier et al. (2003) attempted to apply the CO<sub>2</sub>-slicing method to the VTPR observations in order to extend the observational database back to 1973, but their study stumbled on calibration issues and on significant differences between the HIRS and the VTPR horizontal resolutions. It is most likely that the calibration issues that they discuss actually affected the quality of ERA-40 in the mid-1970s. For the late 1950s, the 1960s, and the early 1970s, only conventional observations exist and they constrain the analysis mainly in the Northern Hemisphere. The lack of validation data parallels the lack of observations to be assimilated. The present study attempts to evaluate the pre-HIRS period of ERA-40 on the basis of the above results for the HIRS period. As in the previous section, clouds are detected in ERA-40 with the simple threshold method defined in section 3c.

The trends for the whole ERA-40 analysis archive are displayed in Figs. 10 and 11. Several interesting features can be noticed. First, the anomaly variability seems to be much reduced before the HIRS observations are available. In particular, the impact of ENSO hardly appears in the tropical eastern Pacific before the 1980s. SST anomalies associated with ENSO events have been larger in the 1980s and 1990s (e.g., Trenberth and Hoar 1997), but the amplitude decrease of the ERA-40 high cloud anomalies for the earlier decades compared to the later ones (from about 10% variations down to about 1%) seems to be much overestimated. Other likely artifacts of the ERA-40 record can be no-

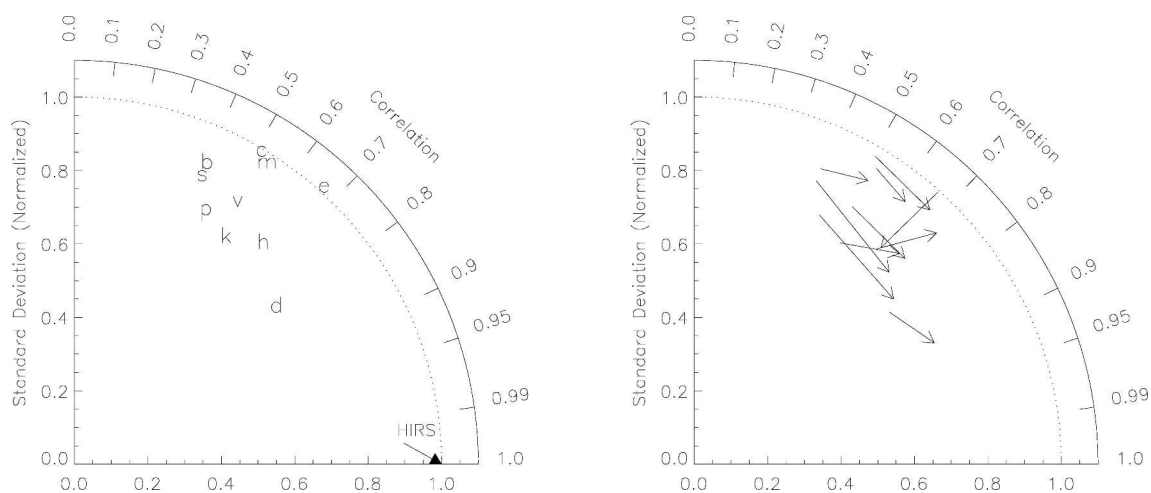


FIG. 9. Polar representation of normalized standard deviations (radius) vs correlations (angle) between the high cloud frequency anomalies from HIRS and ERA-15 (left figure and tail of the arrows in the right figure) or ERA-40 (head of the arrows in the right figure). For both ERA-15 and ERA-40, high clouds are detected from the cloud ice profiles. Monthly anomalies are defined for each dataset with respect to its Jan 1979–Dec 1993 climatology. Statistics are computed for the 10 maritime regions of Table 1.

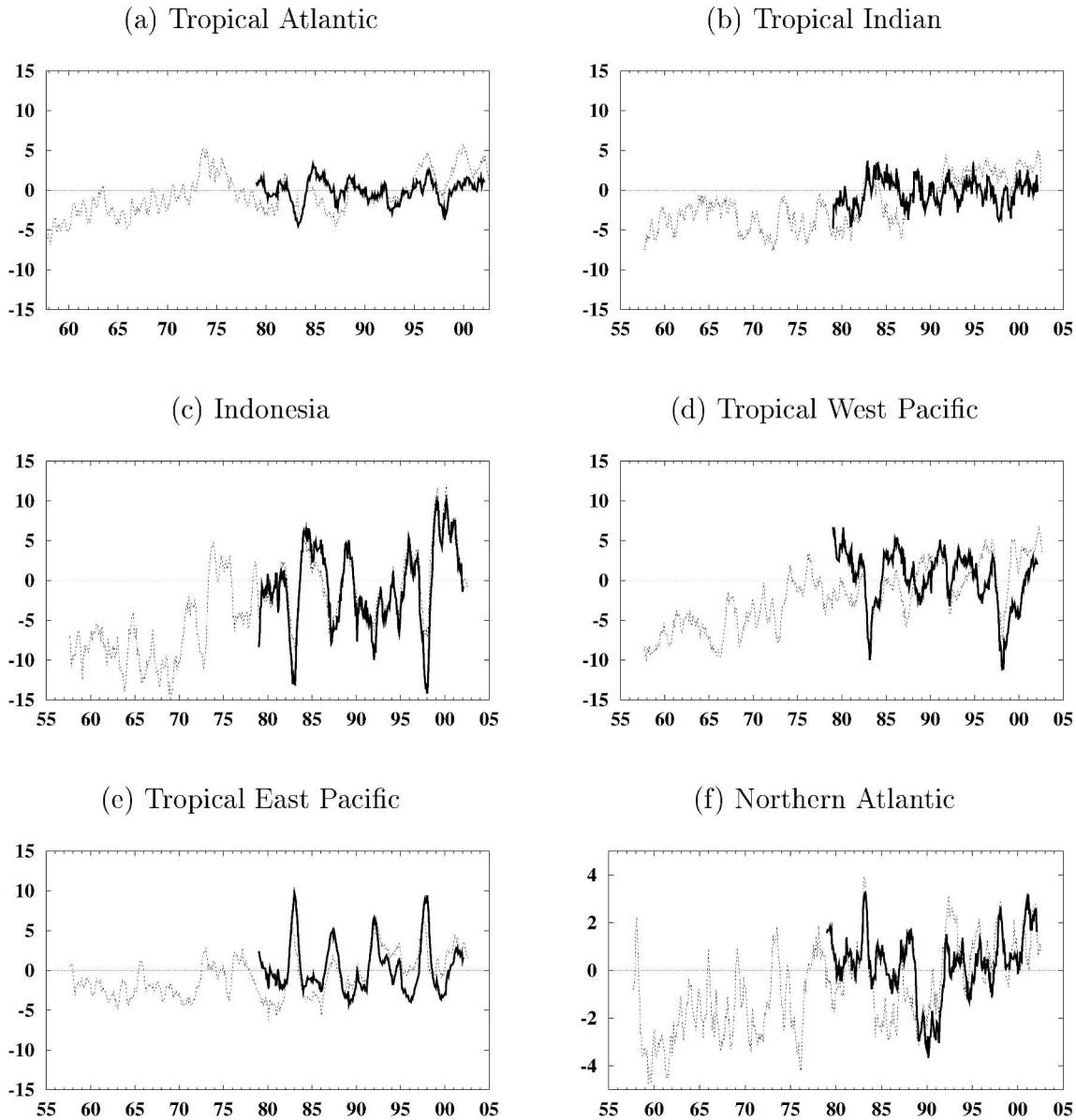


FIG. 10. Mean frequency of high cloud anomalies from ERA-40 analyses (dotted lines) and from HIRS (thick lines) for the first six maritime regions of Table 1. Curves have been smoothed with a two-sided exponentially weighted average. Note that the ordinate scale is smaller in the Tropics. Monthly anomalies are defined for each dataset with respect to its Jan 1979–Feb 2002 climatology. High clouds are detected in the ERA-40 analyses from the cloud ice profiles.

ticed in relation to VTPR in the 1970s. The introduction of VTPR data from *NOAA-2* in January 1973 is accompanied by a sudden increase of high cloudiness by more than 5% in the tropical Indian and Indonesian regions. The erroneous bias correction for the *NOAA-4* VTPR data, mentioned by Chevallier et al. (2003), may have generated the 2% cloudiness decrease in 1975–76 observed in the southern midlatitudes. Lastly, significant variations in the number of available radiosondes before mid-1958 may explain the anomaly drop (by

6%) in ERA-40 during that period in the northern Atlantic.

A complementary assessment of the presatellite period of ERA-40 is provided by the 45-yr climate simulation that was run for the ERA-40 period with the same forecast model and at the same spatial resolution. That simulation was solely forced by the SST, sea ice, and well-mixed greenhouse gas fields and represents the extreme case where no observation is fed to the analysis system. Figure 12 illustrates the seasonal cycle

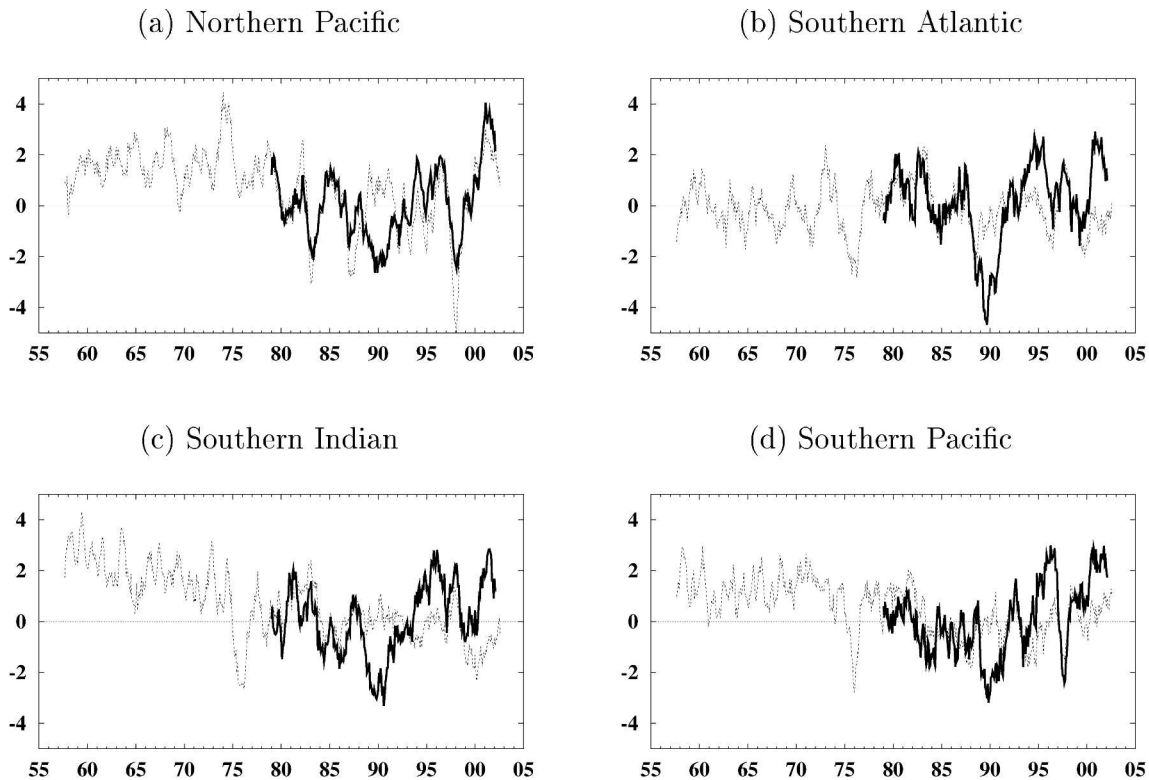


FIG. 11. As in Fig. 10 but for the last four maritime regions of Table 1.

of the run with the mean high cloud frequencies for January and July between July 1983 and September 2001. Annual mean numbers are given in Table 2. That period is chosen to allow the comparison with the HIRS observations of Figs. 3 and 4. Two main features distinguish the high clouds in the climate simulation from the ERA-40 analyses (Figs. 3–4 and 7; Table 2). The first one is the increase of occurrence (between 1.3% and 9.5%) in the extratropics, which makes them closer to the observations. The behavior of the convergence zones in the Indian Ocean and in the western Pacific is the second one. The model ITCZ systematically splits into two branches in the Indian Ocean and the South Pacific convergence zone (SPCZ) separates from the

ITCZ too much westward. Those results actually corroborate known weaknesses of the forecast model (e.g., Jung and Tompkins 2003). In consequence, the climate simulation anomalies, displayed in Fig. 13, do not correlate well with the observations in any of the 10 maritime regions considered.

The imbalance between the analyses and the model physics is noticeable on short-range forecasts as well. For instance, Fig. 14 shows that systematic differences exist between the 36-h forecasts and the analyses: the frequencies of high clouds diminish in the ITCZ away from the analysis, the ITCZ shifts northward in the Atlantic and Pacific Oceans in July, the SPCZ shifts southward in January, and the ITCZ organization var-

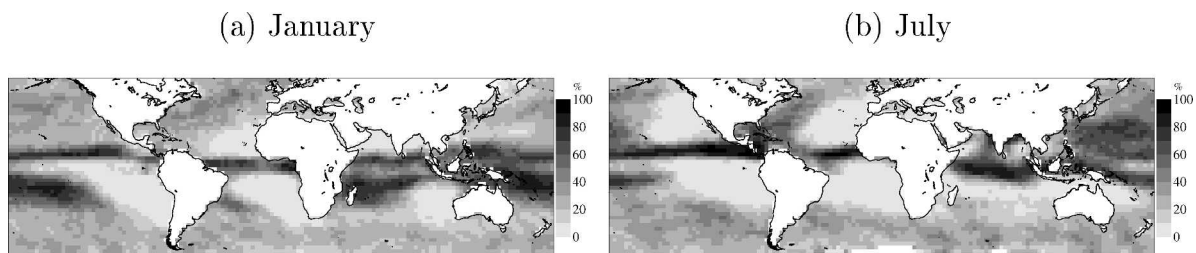


FIG. 12. Mean frequency of high clouds from the climate run for Jan and Jul between Jul 1983 and Sep 2001. High clouds are detected from the cloud ice profiles.

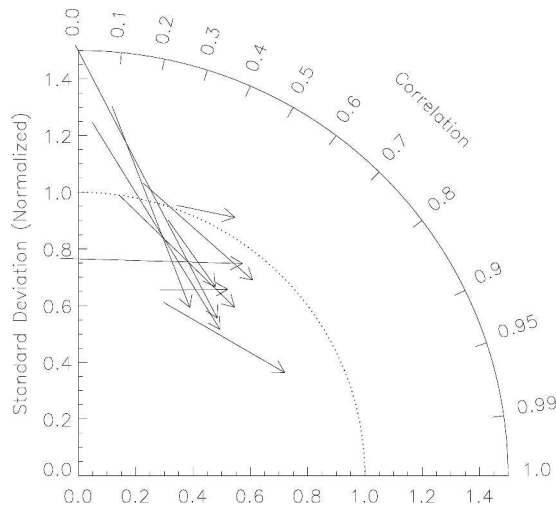


FIG. 13. Polar representation of normalized standard deviations (radius) vs correlations (angle) between the high cloud frequency anomalies from HIRS and the climate run (tail of the arrows) or ERA-40 12-h forecasts (head of the arrows). For the climate run as for ERA-40, high clouds are detected from the cloud ice profiles. Monthly anomalies are defined for each dataset with respect to its Jul 1983–Sep 2001 climatology. Statistics are computed for the 10 maritime regions of Table 1, but for clarity the arrows are not labeled.

ies in the Indian Ocean. It is worth noting that the reduction of high cloud occurrence in the ITCZ is consistent with the known loss of specific humidity by the forecast model during the first hours and days of the integrations, through excessive convective precipitation (Jung and Tompkins 2003).

## 7. Conclusions

The representation of clouds in general, and high ones in particular, has proven to be a challenge for modelers. Furthermore, clouds are not the main focus of ERA-15 and ERA-40 since they are not directly analyzed. Temperature, for instance, is a far more reliable

variable in both reanalyses. However, it is of interest to see how reanalyses perform for less emblematic parameters in order to define their range of possible applications. This study attempted to evaluate ERA-15 and ERA-40 high cloud climatologies over ocean on the basis of HIRS cloud retrievals.

The CO<sub>2</sub>-slicing method of Wylie et al. (1994) has been used to retrieve cloud-top pressures and cloud effective emissivities from HIRS. The constitution of the retrieval dataset already gave some information about the quality of ERA-40 since it used the ERA-40 radiance bias correction. It was shown that the bias correction successfully calibrated the data from many of the instruments uniformly. However, instruments on board 4 of the 11 platforms were not calibrated with the same accuracy. This issue is currently being addressed and improvements should be made for future ECMWF reanalyses.

The ERA-15 and ERA-40 analyses and short-range forecasts have been compared to the HIRS climatology. Consistent with previous validations of the ECMWF model made at various horizontal resolutions and with diverse instruments (Jung and Tompkins 2003, and references therein), the ERA-40 ITCZ is too static and the cloud occurrence is underestimated in the extratropics. It was also found that the seasonal variations around the tropic of Cancer are not adequately represented in the western Pacific and Atlantic Oceans for ERA-40. Despite these weaknesses, ERA-40 dramatically improves on ERA-15 for the realism of the seasonal and interannual variations in high clouds. More than 60% of the observed anomalies during the January 1979–February 2002 period in large oceanic basins are captured by the latest reanalysis.

The quality of high clouds from ERA-40 for the 1960s and the 1970s has been qualitatively assessed. The realism of the analyses in the areas with sparse observations or even none, like the southern oceans or the tropical Pacific in the 1960s, appears to be poor. In

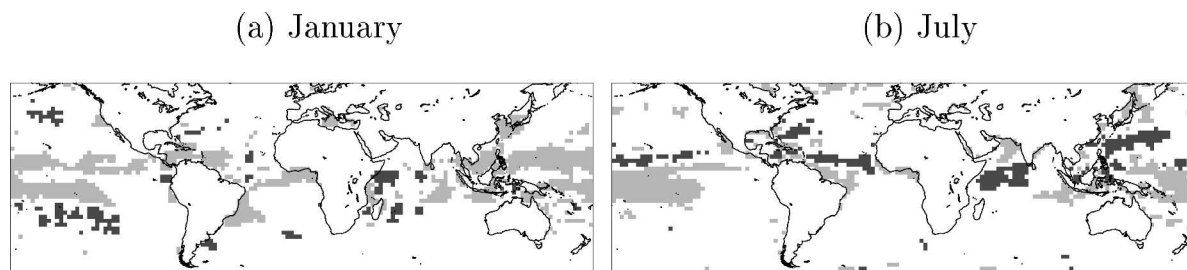


FIG. 14. Difference (forecast–analysis) in high cloud occurrence between ERA-40 36-h forecasts started at 0000 and 1200 UTC and the corresponding 0000 and 1200 UTC analysis for Jan and Jul between Jul 1983 and Sep 2001. Values larger (smaller) than 3% (–3%) are dark (light) shaded. High clouds are detected from the cloud ice profiles.

those regions, the analysis system is mainly driven by the model physics, which was primarily developed for forecasting purposes rather than for long climate runs. In particular, the model radiative budget at the top of the atmosphere is notably poor (Chevallier and Morcrette 2000) despite a good simulation of its clear-sky component (Allan and Ringer 2003). Even for short-range forecasts, systematic differences with the analyses witness the imbalance between the model and the analyses. Moreover, the inadequate calibration of some of the VTPR observations does not make ERA-40 much more reliable in the mid-1970s in those areas where conventional observations are sparse (Chevallier et al. 2003). To summarize, it is unlikely that the ERA-40 interannual variations in most parts of the world can be trusted before 1979.

This study focused on time scales longer than a month and at 2.5° horizontal resolution. We have also evaluated the model radiances for many extratropical cyclones and found no indication of systematic errors, apart from a significant underestimation of the cloud radiation forcing, consistent with the results of Chevallier and Morcrette (2000). However the time-space sampling of the polar orbiters makes it difficult to draw firm conclusions about the quality of synoptic weather systems in ERA-40. The use of geostationary data for validation would be more appropriate. Readers are referred to Chevallier and Kelly (2002) for an evaluation of the ECMWF operational forecasting system with Meteosat radiances. ERA-40 is expected to compare less favorably due to reduced horizontal resolution (125 versus 40 km).

ECMWF will work toward an extensive new reanalysis, which could begin in 2008 or beyond. Already, major changes to the forecasting system are being made to improve the representation of the hydrological cycle (Andersson et al. 2003, 2004). In particular, the assimilation of satellite radiances affected by high clouds is being prepared (Chevallier et al. 2004), which should improve the quality of the upper-tropospheric humidity in the cloud systems. The next reanalysis is expected to significantly benefit from these developments.

*Acknowledgments.* The Satellite Application Facility on Numerical Weather prediction, which is cosponsored by Eumetsat, supported part of this work. The ERA-40 project involved many people at ECMWF and at partner institutes and was partially funded by the European Commission through Contract EVK2-CT-1999-00027. The authors gratefully acknowledge the fruitful interaction with D. P. Wylie and P. Menzel at the University of Wisconsin. They also thank two anonymous reviewers for their constructive comments.

## REFERENCES

- Allan, R. P., and M. A. Ringer, 2003: Inconsistencies between satellite estimates of longwave cloud forcing and dynamical fields from reanalyses. *Geophys. Res. Lett.*, **30**, 1491, doi:10.1029/2003GL017019.
- Andersson, E., A. Beljaars, J. Bidlot, M. Miller, A. Simmons, and J.-N. Thépaut, 2003: A major new cycle of the IFS: Cycle 25r4. *ECMWF Newsletter*, No. 97, ECMWF, Reading, United Kingdom, 12–20.
- , and Coauthors, 2004: Assimilation and modeling of the atmospheric hydrological cycle in the ECMWF forecasting system. *Bull. Amer. Meteor. Soc.*, **86**, 387–402.
- Brest, C. L., W. B. Rossow, and M. D. Roiter, 1997: Update of radiance calibrations for ISCCP. *J. Atmos. Oceanic Technol.*, **14**, 1091–1109.
- Chahine, M. T., 1974: Remote sounding of cloudy atmospheres. I. The single cloud layer. *J. Atmos. Sci.*, **31**, 233–243.
- Chevallier, F., and J.-J. Morcrette, 2000: Comparison of model fluxes with surface and top-of-the-atmosphere observations. *Mon. Wea. Rev.*, **128**, 3839–3852.
- , and G. Kelly, 2002: Model clouds as seen from space: Comparison with geostationary imagery in the 11- $\mu$ m window channel. *Mon. Wea. Rev.*, **130**, 712–722.
- , P. Bauer, G. Kelly, C. Jakob, and T. McNally, 2001: Model clouds over oceans as seen from space: Comparison with HIRS/2 and MSU radiances. *J. Climate*, **14**, 4216–4229.
- , G. Kelly, A. J. Simmons, S. Uppala and A. Hernandez, 2003: High clouds over oceans in the ECMWF 15-year and 45-year re-analyses. ERA-40 Project Report Series 11, 30 pp.
- , P. Lopez, A. M. Tompkins, M. Janisková, and E. Moreau, 2004: The capability of 4D-Var systems to assimilate cloud-affected satellite infrared radiances. *Quart. J. Roy. Meteor. Soc.*, **130**, 917–932.
- Eyre, J. R., 1991: A fast radiative transfer model for satellite sounding systems. ECMWF Tech. Memo. 176, 28 pp.
- Fiorino, M. 2004: A multi-decadal daily sea surface temperature and sea ice concentration data set for the ERA-40 reanalysis. ERA-40 Project Report Series No. 12, 16 pp.
- Gibson, J. K., P. Källberg, S. Uppala, A. Hernandez, A. Nomura, and E. Serrano, 1997: ERA description. Vol. 1, ECMWF Re-analysis, ECMWF Project Report Series, 72 pp.
- Goodrum, G., K. B. Kidwell, and W. Winston, cited 2000: NOAA KLM user's guide. NOAA, NESDIS, NCDC, Climate Services Division, Satellite Services Branch. [Available online at <http://www2.ncdc.noaa.gov/docs/klm/index.htm>.]
- Harris, B. A., and G. Kelly, 2001: A satellite radiance bias correction scheme for radiance assimilation. *Quart. J. Roy. Meteor. Soc.*, **127**, 1453–1468.
- Hernandez, A., G. Kelly, and S. Uppala, 2004: The TOVS/ATOVS observing system in ERA-40. ERA-40 Project Report Series 16, 45 pp.
- Houghton, J. T., Y. Ding, D. J. Griggs, M. Noguer, P. J. van der Linden, X. Dai, K. Maskell, and C. A. Johnson, Eds., 2001: *Climate Change 2001: The Scientific Basis*. Cambridge University Press, 881 pp.
- Hubert, L. F., A. F. Krueger, and J. S. Winston, 1969: The double intertropical convergence zone—Fact or fiction? *J. Atmos. Sci.*, **26**, 771–773.
- Jakob, C., 1999: Cloud cover in the ECMWF reanalysis. *J. Climate*, **12**, 947–959.
- Jin, Y., W. B. Rossow, and D. P. Wylie, 1996: Comparison of the

- climatologies of high-level clouds from HIRS and ISCCP. *J. Climate*, **9**, 2850–2879.
- Jung, T., and A. Tompkins, 2003: Systematic errors in the ECMWF forecasting system. ECMWF Tech. Memo. 422, 72 pp.
- Kidwell, K. B., cited 1998: NOAA polar orbiter data user's guide. Tech. Rep., NOAA, NESDIS, NCDC, Climate Services Division, Satellite Services Branch. [Available online at <http://www2.ncdc.noaa.gov/docs/podug/index.htm>.]
- Liao, X., W. B. Rossow, and D. Rind, 1995: Comparison between SAGE II and ISCCP high-level clouds: 1. Global and zonal mean cloud amounts. *J. Geophys. Res.*, **100**, 1121–1135.
- Liebmann, B., G. N. Kiladis, J. A. Marengo, T. Ambrizzi, and J. D. Glick, 1999: Submonthly convective variability over South America and the South Atlantic convergence zone. *J. Climate*, **12**, 1877–1891.
- Luo, Z., W. B. Rossow, T. Inoue, and C. J. Stubenrauch, 2002: Did the eruption of the Mt. Pinatubo volcano affect cirrus properties? *J. Climate*, **15**, 2806–2820.
- Morcrette, J.-J., E. J. Mlawer, M. J. Iacono, and S. A. Clough, 2001: Impact of the radiation-transfer scheme RRTM in the ECMWF forecasting system. *ECMWF Newsletter*, No. 91, ECMWF, Reading, United Kingdom, 2–9.
- Price, J. C., 1991: Timing of NOAA afternoon passes. *Int. J. Remote Sens.*, **12**, 193–198.
- Rossow, W. B., and R. A. Schiffer, 1999: Advances in understanding clouds from ISCCP. *Bull. Amer. Meteor. Soc.*, **80**, 2261–2287.
- Saunders, R., M. Matricardi, and P. Brunel, 1999: An improved fast radiative transfer model for assimilation of satellite radiance observations. *Quart. J. Roy. Meteor. Soc.*, **125**, 1407–1425.
- Scott, N. A., and Coauthors, 1999: Characteristics of the TOVS Pathfinder Path-B database. *Bull. Amer. Meteor. Soc.*, **80**, 2679–2702.
- Simmons, A. J., 2001: Development of the ERA-40 data assimilation system. Workshop on Re-analysis, 5–9 November 2001, Vol. 3, ERA-40 Project Report Series, 11–30.
- , and J. K. Gibson, Eds., 2000: The ERA-40 project plan. ERA-40 Project Report Series 1, 62 pp.
- , and A. Hollingsworth, 2002: Some aspects of the improvement of skill of numerical weather prediction. *Quart. J. Roy. Meteor. Soc.*, **128**, 647–677.
- Smith, W. L., H. M. Woolf, C. M. Hayden, D. Q. Wark, and L. M. McMillin, 1979: The TIROS-N operational vertical sounder. *Bull. Amer. Meteor. Soc.*, **60**, 1177–1187.
- Stubenrauch, C. J., W. B. Rossow, F. Chérut, A. Chédin, and N. A. Scott, 1999: Clouds as seen by satellite sounders (3I) and imagers (ISCCP). Part I: Evaluation of cloud parameters. *J. Climate*, **12**, 2189–2213.
- Susskind, J., P. Piraino, L. Rokke, L. Iredell, and A. Mehta, 1997: Characteristics of the TOVS Pathfinder Path A dataset. *Bull. Amer. Meteor. Soc.*, **78**, 1449–1472.
- Taylor, K. E., 2001: Summarizing multiple aspects of model performance in a single diagram. *J. Geophys. Res.*, **106**, 7183–7192.
- Tiedtke, M., 1993: Representation of clouds in large-scale models. *Mon. Wea. Rev.*, **121**, 3040–3061.
- Trenberth, K. E., and T. J. Hoar, 1997: El Niño and climate change. *Geophys. Res. Lett.*, **24**, 3057–3060.
- Wylie, D. P., and P.-H. Wang, 1997: Comparison of cloud frequency data from the High-resolution Infrared Radiometer Sounder and the Stratospheric Aerosol and Gas Experiment II. *J. Geophys. Res.*, **102**, 29 893–29 900.
- , and W. P. Menzel, 1999: Eight years of high cloud statistics using HIRS. *J. Climate*, **12**, 170–184.
- , —, H. M. Woolf, and K. I. Strabala, 1994: Four years of global cirrus cloud statistics using HIRS. *J. Climate*, **7**, 1972–1986.